
Wasserstein Dependency Measure for Representation Learning

Sherjil Ozair^{1,2} Corey Lynch² Yoshua Bengio¹ Aäron van den Oord³ Sergey Levine² Pierre Sermanet²

Abstract

Mutual information maximization has emerged as a powerful learning objective for unsupervised representation learning obtaining state-of-the-art performance in applications such as object recognition, speech recognition, and reinforcement learning. However, such approaches are fundamentally limited since a tight lower bound on mutual information requires sample size exponential in the mutual information. This limits the applicability of these approaches for prediction tasks with high mutual information, such as in video understanding or reinforcement learning. In these settings, such techniques are prone to overfit, both in theory and in practice, and capture only a few of the relevant factors of variation. This leads to incomplete representations that are not optimal for downstream tasks. In this work, we empirically demonstrate that mutual information-based representation learning approaches do fail to learn complete representations on a number of designed and real-world tasks. To mitigate these problems we introduce the Wasserstein dependency measure, which learns more complete representations by using the Wasserstein distance instead of the KL divergence in the mutual information estimator. We show that a practical approximation to this theoretically motivated solution, constructed using Lipschitz constraint techniques from the GAN literature, achieves substantially improved results on tasks where incomplete representations are a major challenge.

1. Introduction

Recent success in supervised learning can arguably be attributed to the paradigm shift from engineering representations to learning representations (LeCun et al., 2015). Especially in the supervised setting, effective representations

can be acquired directly from the labels. However, representation learning in the unsupervised setting, without hand-specified labels, becomes significantly more challenging: although much more data is available for learning, this data lacks the clear learning signal that would be provided by human-specified semantic labels. Nevertheless, unsupervised representation learning has made significant progress recently, due to a number of different approaches. Representations can be learned via implicit generative methods (Goodfellow et al., 2014; Dumoulin et al., 2016; Donahue et al., 2016; Odena et al., 2017), via explicit generative models (Kingma & Welling, 2013; Rezende & Mohamed, 2015; Dinh et al., 2016; Rezende & Mohamed, 2015; Kingma et al., 2016), and self-supervised learning (Becker & Hinton, 1992; Doersch et al., 2015; Zhang et al., 2016; Doersch & Zisserman; van den Oord et al., 2018; Wei et al., 2018; Hjelm et al., 2018). Among these, the latter methods are particularly appealing because they remove the need to actually generate full observations (e.g., image pixels or audio waveform). Self-supervised learning techniques have demonstrated state-of-the-art performance in speech and image understanding (van den Oord et al., 2018; Hjelm et al., 2018), reinforcement learning (Jaderberg et al., 2016; Dwibedi et al., 2018; Kim et al., 2018), imitation learning (Sermanet et al., 2017; Aytar et al., 2018), and natural language processing (Devlin et al., 2018; Radford et al.).

Self-supervised learning techniques make use of discriminative *pretext* tasks, chosen in such a way that its labels can be extracted automatically and such that solving the task requires a semantic understanding of the data, and therefore a meaningful representation. For instance, Doersch et al. (2015) predict the relative position of adjacent patches extracted from an image. Zhang et al. (2016) reconstruct images from their grayscale versions. Gidaris et al. (2018) predict the canonically upwards direction in rotated images. Sermanet et al. (2017) maximize the mutual information between two views of the same scene. Hjelm et al. (2018) maximize mutual information between an image and patches of the image.

However, a major issue with such techniques is that the pretext task must not admit trivial or easy solutions. For instance, Doersch et al. (2015) found that relative position could be easily predicted using low-level cues such as boundary patterns, shared textures, long edges, and even chromatic

¹MILA, Université de Montréal ²Google Brain ³Deepmind, London. Correspondence to: Sherjil Ozair <sherjilozair@gmail.com>.

Exploit	Fix
Boundary pattern	Gap between patches
Shared textures	gap between patches
Long edges	Jitter
Chromatic aberration	Grayscaleing
Black framing	Cropping
Cinematic camera motion	Stabilization
Dominant agent and objects	-

Table 1. An inexhaustive list of exploits and their corresponding fixes used in self-supervised representation learning methods. Semi-supervised learning methods are known to perform poorly when the model can “cheat” by exploiting syntactic patterns which don’t help learn good representations.

aberration. In some cases such as these, trivial solutions are easily identifiable and rectified, such as by adding gaps between patches, adding random jitter, and/or grayscaleing the patches. Table 1 lists some of these tricks used in self-supervised learning.

Identifying such exploits and finding fixes is a cumbersome process, requires expert knowledge about the domain, and can still fail to eliminate all degenerate solutions. However, even when care is taken to remove such low-level regularities, self-supervised representation learning techniques can still suffer and produce incomplete representations, i.e. representations that capture only a few of the underlying factors of variations in the data.

Recent work has provided a theoretical underpinning of this empirically observed shortcoming. A number of self-supervised learning techniques can be shown to be maximizing a lower bound to mutual information between representations of different data modalities (Belghazi et al., 2018; van den Oord et al., 2018; Poole et al., 2018). However, as shown by McAllester & Statos (2018), lower bounds to the mutual information are only tight for sample size exponential in the mutual information. Unfortunately, many practical problems of interest where representation learning would be beneficial have large mutual information. For instance, mutual information between successive frames in a temporal setting scales with the number of objects in the scene. Self-supervised learning techniques in such settings often only capture a few objects since modeling a few objects is sufficient to confidently predict future frames from a random sample of frames.

In this paper, we motivate this limitation formally in terms of the fundamental limitations of mutual information estimation and KL divergences, and show examples of this limitation empirically, illustrating relatively simple problems where fully reconstructive models can easily learn complete representations, while self-supervised learning methods struggle. We then propose a potential solution to

this problem, by employing the Wasserstein metric in place of KL divergence as a training objective. In practice, we show that approximating this by means of recently proposed regularization methods designed for generative adversarial networks can substantially reduce the incomplete representation problem, leading to a substantial improvement in the ability of representations learned via mutual information estimation to capture task-salient features.

2. Background

In this section, we review some of the concepts we will be referencing throughout the paper: representation learning, mutual information, and Wasserstein distance.

2.1. Representation Learning

The goal of supervised learning is to learn a model $p(y|x)$. Here x could be real-valued high-dimensional vectors representing the raw contents of an image, an audio waveform, or sensory data in general, and y could be a low-dimensional vector representing a label in the case of classification.

A *representation encoder* is a function $f : \mathbb{R}^D \rightarrow \mathbb{R}^d$, where $z = f(x)$ is a *representation* of the underlying data sample x . Typically, the dimensionality of the representation z is much smaller than the dimensionality of x , i.e., $d \ll D$. The goal of representation learning is to learn a representation encoder such that using the representation instead of the raw input helps with the downstream learning task, i.e. $p(y|z = f(x))$ is easier to learn than $p(y|x)$. This could be by improving the generalization, sample efficiency, or compute efficiency of the downstream learning task.

2.2. Mutual Information

Mutual information is a dependency measure between two random variables. For random variables x and y , the mutual information is the Kullback-Leibler divergence between the joint distribution $p(x, y)$ and the product of marginal distributions $p(x)p(y)$,

$$\begin{aligned} I(X; Y) &= KL(p(x, y) || p(x)p(y)) \\ &= \mathbb{E}_{p(x, y)} \left[\log \left(\frac{p(x, y)}{p(x)p(y)} \right) \right] \end{aligned} \quad (1)$$

The mutual information is zero when the random variables are independent, and is infinite when the random variables are identical.

2.3. Wasserstein Distance

The Wasserstein distance between two densities $p(x)$ and $q(y)$ with support on a compact metric space (\mathcal{M}, d) is

defined as

$$\mathcal{W}(p, q) \stackrel{\text{def}}{=} \inf_{\gamma \in \Gamma(p, q)} \int_{\mathcal{M} \times \mathcal{M}} d(x, y) d\gamma(x, y) \quad (2)$$

Here $\Gamma(p, q)$ is the set of all possible *couplings* of the densities p and q .

A joint distribution $\gamma(x, y)$ is a *coupling* of p and q iff $\int_{\mathcal{M}} \gamma(x, y) dy = p(x)$ and $\int_{\mathcal{X}} \gamma(x, y) dx = q(y)$.

Wasserstein distance also has an alternative form due to the Kantorovich-Rubenstein duality (Villani, 2008).

$$\mathcal{W}(p, q) = \sup_{f \in \mathcal{L}_{\mathcal{M}}} \mathbb{E}_{p(x)}[f(x)] - \mathbb{E}_{q(x)}[f(x)] \quad (3)$$

Here, $\mathcal{L}_{\mathcal{M}}$ is the set of all 1-Lipschitz functions in $\mathcal{M} \rightarrow \mathbb{R}$. A function $f : \mathcal{M} \rightarrow \mathbb{R}$ is 1-Lipschitz if for any $x, y \in \mathcal{M}$, we have $f(x, y) \leq d(x, y)$.

The theory of optimal transport from which Wasserstein distances emerge has a long history. For a rigorous and exhaustive treatment we refer the reader to Peyré et al. (2017) and Villani (2008).

3. Mutual Information Estimation and Maximization

Mutual information for representation learning has a long history. One approach (Linsker, 1988; Bell & Sejnowski, 1995) is to maximize the mutual information between observed data samples x and learned representations $z = f(x)$, i.e. $I(x; z)$, thus ensuring the representation learned retain the most information about the underlying data. Another (Becker & Hinton, 1992) is to maximize the mutual information between representations of two different modalities of the data, i.e. $I(f(x); f(y))$.

However, such representation learning approaches have been limited due to the difficulty of estimating mutual information. Previous approaches have had to make parametric assumptions about the data or use nonparametric approaches (Kraskov et al., 2004; Nemenman et al., 2004) which don't scale well to high-dimensional data.

More recently Nguyen et al. (2010), Belghazi et al. (2018), van den Oord et al. (2018), and Poole et al. (2018) have proposed variational energy-based lower bounds to the mutual information which are tractable in high dimension and can be estimated by gradient-based optimization, which makes them suitable to combine with deep learning.

While Becker & Hinton (1992) had chosen to maximize mutual information between representations of spatially adjacent patches of an image, one can also use past and future states such as shown recently by van den Oord et al. (2018) and Sermanet et al. (2017) which has connections to predictive coding in speech (Atal & Schroeder, 1970;

Elias, 1955), predictive processing in the brain (Clark, 2013; Palmer et al., 2015; Tkačik & Bialek, 2016) and the free energy principle (Friston & Kiebel, 2009).

These techniques have shown promising results, but their applicability is still limited to low mutual information settings.

3.1. Formal Limitations in Mutual Information Estimation

The limitations in estimating mutual information via lower bounds stems from those of the KL divergence. Theorem 1 formalizes this limitation of estimating the KL divergence via lower bounds. This result is based on the derivation by McAllester & Statos (2018), who prove a stronger claim for the case where $p(x)$ is fully known.

Theorem 1. *Let $p(x)$ and $q(x)$ be two distributions, and $R = \{x_i \sim p(x)\}_{i=1}^n$ and $S = \{x_i \sim q(x)\}_{i=1}^n$ be two sets of n samples from $p(x)$ and $q(x)$ respectively. Let δ be a confidence parameter, and let $B(R, S, \delta)$ be a real-valued function of the two samples S and R and the confidence parameter δ .*

We have that, if with probability at least $1 - \delta$,

$$B(R, S, \delta) \leq KL(p(x) || q(x))$$

then with probability at least $1 - 4\delta$ we have

$$B(R, S, \delta) \leq \log n.$$

Thus, since the mutual information corresponds to KL divergence, we can conclude that any high-confidence lower bound on the mutual information requires $n = \exp(I(x; y))$, i.e., sample size exponential in the mutual information.

4. Wasserstein Dependency Measure

The KL divergence is not only problematic for representation learning due to the statistical limitations described in Theorem 1, but also due to its property of being completely agnostic to the metric of the underlying data distribution, and invariant to any invertible transformation. KL divergence is sensitive to small differences in the data samples. When used for representation learning, the encoder can often only represent small parts of the data samples, since any small differences found is sufficient to maximize the KL divergence. The Wasserstein distance, however, is a metric-aware divergence, and represents the difference between two distributions in terms of the actual distance between data samples. A large Wasserstein distance actually represents large distances between the underlying data samples. On the other hand, KL divergence can be large even if the underlying data samples differ very little.

This qualitative difference between the KL divergence and Wasserstein distance was recently noted by Arjovsky et al. (2017) to propose the Wasserstein GAN, a metric-aware extension to the original GAN proposed by Goodfellow et al. (2014) which is based on the Jensen symmetrization of the KL divergence (Crooks, 2017). For GANs, we would like the discriminator to model not only the density ratio of two distributions, but the complete process of how one distribution can be transformed into another, which is the underlying basis of the theory of optimal transport and Wasserstein distances (Villani, 2008).

This motivates us to investigate the use of the Wasserstein distance as a replacement for the KL divergence in mutual information, which we call *Wasserstein dependency measure*.

Definition 4.1. Wasserstein dependency measure. For two random variables x and y with joint distribution $p(x, y)$, we define the Wasserstein dependency measure $I_{\mathcal{W}}(x; y)$ as the Wasserstein distance between the joint distribution $p(x, y)$ and the product of marginal distributions $p(x)p(y)$.

$$I_{\mathcal{W}}(x; y) \stackrel{\text{def}}{=} \mathcal{W}(p(x, y), p(x)p(y)) \quad (4)$$

Thus, the Wasserstein dependency measure (WDM) measures the cost of transforming samples from the marginals to samples from the joint, and as such, has to model the generative process of doing so. This is unlike a KL divergence which doesn't have a similar generative component, and only has to discriminate how two distributions differ.

4.1. Choice of Metric Space

The Wasserstein dependency measure assumes that the data lies in a known metric space. However, the purpose of representation learning is often to use the representations to implicitly form a metric space for the data. Thus, it may seem that we're assuming the solution by requiring knowledge of the metric space. However, the difference between the two is that the base metric used in the Wasserstein distance is data-independent, while the metric induced by the representations is informed by the data. The two metrics can be thought of as prior and posterior metrics. Thus, the base metric should encode our prior beliefs about the task independent of the data samples, which acts as inductive bias to help learn a better posterior metric induced by the learned representations. In our experiments we assume a Euclidean metric space for all the tasks.

4.2. Generalization of Wasserstein Distances

Theorem 1 is a statement about mutual information lower bound's inability to generalize for large values, since the gap between the lower bound sample estimate and the true mutual information is not bounded. The Wasserstein dis-

tance, however, can be shown to have better generalization properties when used with Lipschitz neural net function approximation via its dual representation. Neyshabur et al. (2017) show that a neural network's generalization gap is proportional to the square root of the network's Lipschitz constant, which is bounded ($= 1$) for the function class used in Wasserstein distance estimation, but is unbounded for the function class used in mutual information lower bounds.

5. Wasserstein Predictive Coding for Representation learning

Estimating Wasserstein distances is intractable in general. We will use the Kantorovich-Rubenstein duality (Villani, 2008), as stated in Equation 3, to obtain the dual form of the Wasserstein dependency measure, which allows for easier estimation since the dual form allows gradient-based optimization over the function space using neural networks.

$$\begin{aligned} I_{\mathcal{W}}(x; y) &\stackrel{\text{def}}{=} \mathcal{W}(p(x, y), p(x)p(y)) \\ &= \sup_{f \in \mathcal{L}_{\mathcal{M} \times \mathcal{M}}} \mathbb{E}_{p(x, y)}[f(x, y)] - \mathbb{E}_{p(x)p(y)}[f(x, y)] \end{aligned} \quad (5)$$

Here, $\mathcal{L}_{\mathcal{M} \times \mathcal{M}}$ is the set of all 1-Lipschitz functions in $\mathcal{M} \times \mathcal{M} \rightarrow \mathbb{R}$.

We note that Equation 3 is similar to contrastive predictive coding (CPC) van den Oord et al. (2018), which optimizes

$$\begin{aligned} \mathcal{J}_{CPC} &= \sup_{f \in \mathcal{F}} \mathbb{E}_{p(x, y)p(y_j)} \left[\log \frac{\exp f(x, y)}{\sum_j \exp f(x, y_j)} \right] \\ &= \sup_{f \in \mathcal{F}} \mathbb{E}_{p(x, y)}[f(x, y)] \\ &\quad - \mathbb{E}_{p(x)p(y_j)} \left[\log \sum_j \exp f(x, y_j) \right]. \end{aligned} \quad (6)$$

The two main differences between contrastive predictive coding and the dual Wasserstein dependency measure is the Lipschitz constraint on the function class and the $\log \sum \exp$ in the second term of CPC.

We propose a new objective, which is a lower bound on both contrastive predictive coding and the dual Wasserstein dependency measure, by keeping both the Lipschitz class of functions and the $\log \sum \exp$, which we call Wasserstein predictive coding (WPC):

$$\begin{aligned} \mathcal{J}_{WPC} &= \sup_{f \in \mathcal{L}_{\mathcal{M} \times \mathcal{M}}} \mathbb{E}_{p(x, y)}[f(x, y)] \\ &\quad - \mathbb{E}_{p(x)p(y_j)} \left[\log \sum_j \exp f(x, y_j) \right]. \end{aligned} \quad (7)$$

We choose to keep the $\log \sum \exp$ since it decreases the variance when we use samples to estimate the gradient, which we found to improve performance in practice. In the previous sections, we motivated the use of Wasserstein distance, which directly suggests the use of a Lipschitz constraint in Equation 7. Below, we also provide a more intuitive justification for the Lipschitz constraint:

CPC and similar contrastive learning techniques work by reducing the distance between paired samples, and increasing the distance between unpaired random samples. However, when using powerful neural networks as the representation encoder, the neural network can learn to exaggerate small differences between unpaired samples to increase the distance between arbitrarily. This then prevents the encoder to learn any other differences between unpaired samples because one discernible difference suffices to optimize the objective. However, if we force the encoder to be Lipschitz, then the distance between learned representations is bounded by the distance between the underlying samples. Thus, to optimize the objective, the encoder is forced to represent more components of the data.

5.1. Approximating Lipschitz Continuity

Optimization over Lipschitz functions with neural networks is a challenging problem, and a topic of active research. Due to the popularity of the Wasserstein GAN (Arjovsky et al., 2017), a number of techniques have been proposed to approximate Lipschitz continuity (Gulrajani et al., 2017; Miyato et al., 2018). However, recent work (Anil et al., 2018) has shown that neural networks that use elementwise monotonically increasing 1-Lipschitz activation functions (such as ReLU) are not universal Lipschitz function approximators. For these type of neural networks, Lipschitz continuity significantly reduces the nonlinear capacity of the neural network, which could hurt performance in complex tasks where high capacity neural networks are essential. This is also observed by Brock et al. (2018) in the context of training GANs.

Thus, in our experiments, we use the gradient penalty technique proposed by Gulrajani et al. (2017), which is sufficient to provide experimental evidence in support of our hypothesis, but we note the caveat that gradient penalty combined with ReLU networks might not be effective for complex tasks. Incorporating better and more scalable methods to enforce Lipschitz continuity would likely further improve practical WDM implementations.

6. Experiments

The goal of our experiments are the following:

- To demonstrate and quantify the limitations of mutual

information-based representation learning.

- To quantitatively compare our proposed alternative, the Wasserstein dependency measure, with mutual information for representation learning.
- To demonstrate the importance of the class of functions being used to practically approximate dependency measures, such as fully-connected or convolutional networks.

6.1. Evaluation Methodology

All of our experiments make use of datasets generated via the following process: $p(z)p(x, y|z)$. Here, z is the underlying latent variable, and x and y are observed variables. In our experiments, z is always a discrete variable, and x and y are images. We specifically use datasets with large values of the mutual information $I(x; y)$, which is common in practice and is also the condition under which we expect current MI estimators to struggle.

The goal of the representation learning task is to learn representation encoders $f \in \mathcal{F}$ and $g \in \mathcal{F}$, such that the representations $f(x)$ and $g(y)$ capture the underlying generative factors of variation represented by the latent variable z . For instance, for SpatialMultiOmniglot (described in 6.2), we want that $f(x)$ captures the class of each of the characters in the image. However, representation learning is not about making sure the representations contain the requisite information, but that they contain the requisite information in an accessible way, ideally, via linear probes (Alain & Bengio, 2016). Thus, we measure the quality of the representations by learning linear classifiers predicting the underlying latent variables z . This methodology is standard in the self-supervised representation learning literature.

6.2. Task Design

We present experimental results on four tasks, SpatialMultiOmniglot, StackedMultiOmniglot, MultiviewShapes3D, and SplitCelebA.

SpatialMultiOmniglot. We used the Omniglot dataset (Lake et al., 2015) as a base dataset to construct SpatialMultiOmniglot and StackedMultiOmniglot. SpatialMultiOmniglot is a dataset of paired images x and y , where x is an image of size $(32m, 32n)$ comprised of mn Omniglot character arranged in a (m, n) grid from different Omniglot alphabets, as illustrated in Figure 1. The characters in y are the next characters of the corresponding characters in x , and the latent variable z is the index of each of the characters in x .

Let l_i be the alphabet size for the i^{th} character in x . The mutual information $I(x; y)$ is $\sum_{i=1}^{mn} \log l_i$. Thus, adding

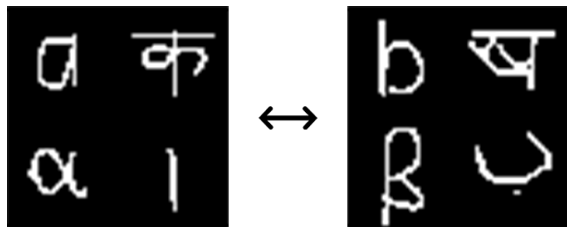


Figure 1. The SpatialMultiOmniglot dataset consists of pairs of images (x, y) each comprising of multiple Omniglot characters in a grid, where the characters in y are the next characters in the alphabet of the characters in x .

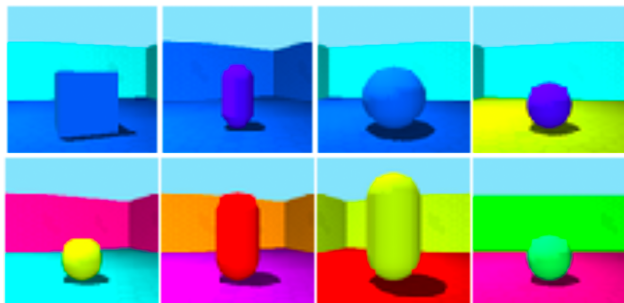


Figure 2. The Shapes3D dataset is a collection of colored images of an object in a room. Each image corresponds to a unique value for the underlying latent variables: color of object, color of wall, color of floor, shape of object, size of object, viewing angle. To construct the Multiview Shapes3D task, we pick two extreme viewing angles, and consider images which share all other latent variables to be samples from the joint $p(x, y)$, i.e. x and y share all latent variables except the viewing angle.

more characters increases the mutual information and easily allows to control the complexity of the task.

For our experiments, we picked the 9 largest alphabets which are Tifnagh [55], Japanese (hiragana) [52], Gujarati [48], Japanese (katakana) [47], Bengali [46], Grantha [43], Sanskrit [42], Armenian [41], and Mkhedruli (Georgian) [41], with their respective alphabet sizes in square brackets.

StackedMultiOmniglot. StackedMultiOmniglot is similar to SpatialMultiOmniglot except the characters are stacked in the channel axis, and thus x and y are arrays of size $(32, 32, n)$. This dataset is designed to remove feature transfer between characters of different alphabets that is present in SpatialMultiOmniglot when using convolutional neural networks. The mutual information is the same, i.e. $I(x; y) \sum_{i=1}^n \log l_i$.

MultiviewShapes3D. Shapes3D (Kim & Mnih, 2018) (Figure 2) is a dataset of images of a single object in a room. It has six factors of variation: object color, wall



Figure 3. The SplitCelebA dataset consists of pairs of images $p(x, y)$ where x and y are the left and right halves of the same CelebA image, respectively.

color, floor color, object shape, object size, and camera angle. These factors have 10, 10, 10, 4, 6, and 15 values respectively. Thus, the total entropy of the dataset is $\log(10 \times 10 \times 10 \times 4 \times 6 \times 15)$. MultiviewShapes3D is a subset of Shapes3D where we select only the two extreme camera angles for x and y , and the other 5 factors of x and y comprise the latent variable z .

SplitCelebA. CelebA (Liu et al., 2015) is a dataset consisting of celebrity faces. The SplitCelebA task uses samples from this dataset split into left and right halves. Thus x is the left half, and y is the right half. We use the CelebA binary attributes as the latent variable z .

6.3. Effect of Mutual Information

Our first main experimental contribution is to show the effect of dataset size on the performance of mutual information-based representation learning, in particular, of contrastive predictive coding (CPC).

Figure 4(c) shows the performance of CPC and WPC as the mutual information increases. We were able to control the mutual information in the data by controlling the number of characters in the images. We kept the training dataset size fixed at 50,000 samples. This confirms our hypothesis that mutual information-based representation learning indeed suffers when the mutual information is large. As can be seen, for small number (1 and 2) of characters, CPC has near-perfect representation learning. The exponential of the mutual information in this case is 55 and $55 \times 52 = 2860$ (i.e. the product of alphabet class sizes), which is smaller than the dataset size. However, when the number of characters is 3, the exponential of the mutual information is $55 \times 52 \times 48 = 137280$ which is larger than the dataset size. This is the case where CPC is no longer a good lower bound estimator for the mutual information, and the representation learning performance drops down significantly.

We observe that while WPC's performance also drops when the mutual information is increased, however it's always

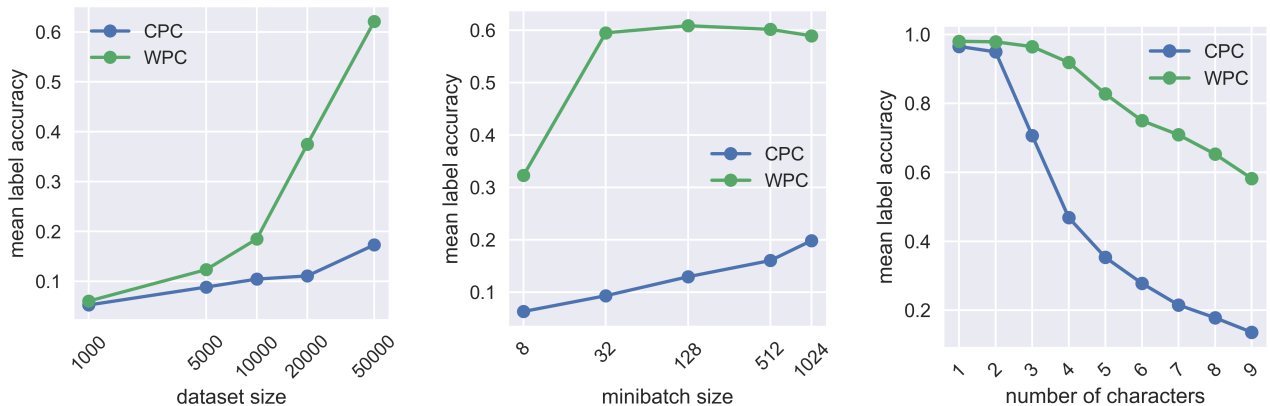


Figure 4. Performance of CPC and WPC on StackedMultiOmniglot using fully connected neural networks. Note that WPC performs better than CPC for multiple dataset sizes. CPC’s performance is influenced by batch size, while WPC’s performance is more robust to minibatch size, while being consistently better. When number of characters is increased (which increases the mutual information $I(x; y)$), CPC’s performance drops drastically when $\log I(x; y)$ is larger than dataset size, while WPC is more robust, and performs consistently better.

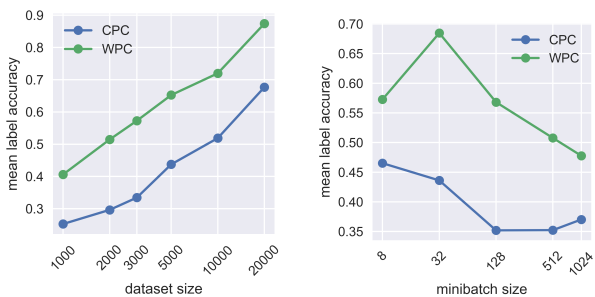


Figure 5. Performance of CPC and WPC on MultiviewShapes3D using fully connected neural networks. WPC performs consistently better than CPC for multiple dataset and minibatch sizes.

better than CPC, and the drop in performance is more gradual. Ideally, representation learning performance should not be effected by the number of characters at all. We believe WPC’s less-than-ideal performance is due to the practical approximations we used such as gradient penalty.

6.4. Effect of Dataset Size

Figures 4(a), and 5(a) show the performance of CPC and WPC as we vary the dataset size. For the Omniglot datasets, the number of characters has been fixed to 9, and the mutual information for this dataset is the logarithm of the product of the 9 alphabet sizes which is around 34.43 nats. This is a very large information value as compared to the dataset size, and thus, we observe that the performance of either method is far from perfect. However, WPC performs significantly better than CPC.

Method	CelebA
CPC (fc)	0.85
WPC (fc)	0.87
CPC (convnet)	0.82
WPC (convnet)	0.87

Table 2. Performance of CPC and WPC on SplitCelebA dataset using fully connected and convolutional networks. WPC’s performance doesn’t depend on the function class being used and is better than CPC.

6.5. Effect of Minibatch Size

Both CPC and WPC are minibatch-dependent techniques. For small mininatches, the variance of the estimator becomes large. We observe in Figure 4(b) that CPC’s performance increases as the minibatch size is increased. However, WPC’s performance is not as sensitive on the minibatch size. WPC reaches its optimal performance with a minibatch size of 32, and any further increase in minibatch size does not improve the performance. Thus, we conclude that Wasserstein-based representation learning is effective even at small minibatch sizes.

6.6. Effect of Neural Network Inductive Bias

Use of fully connected neural networks allowed us to make predictions about the performance based on whether the mutual information is larger or smaller than the log dataset size. However, most practical uses of representation learning use convolutional neural networks (convnet). Convnets change the interplay of mutual information and dataset sizes, since they can be more efficient with smaller dataset sizes

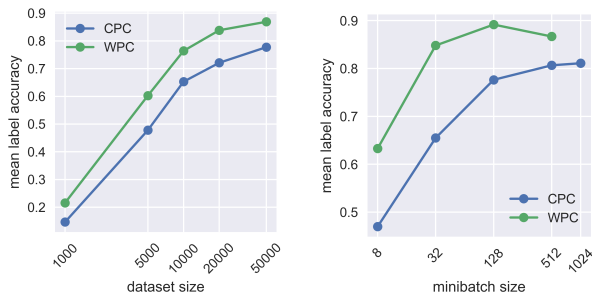


Figure 6. Performance of CPC and WPC on SpatialMultiOmniglot using convolutional neural networks. While using CNNs does improve CPC’s performance, WPC still consistently performs better across many dataset and minibatch sizes. However the difference in performance, since SpatialMultiOmniglot has a spatial structure which suits CNNs well.

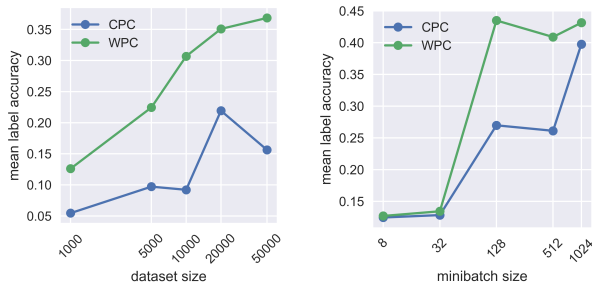


Figure 7. Performance of CPC and WPC on StackedMultiOmniglot using convolutional neural networks. The performance gap between CPC and WPC widens when using a dataset structure which does not suit CNNs well. Thus, WPC is likely to help when the prior induced by the function class does not ideally suit the dataset.

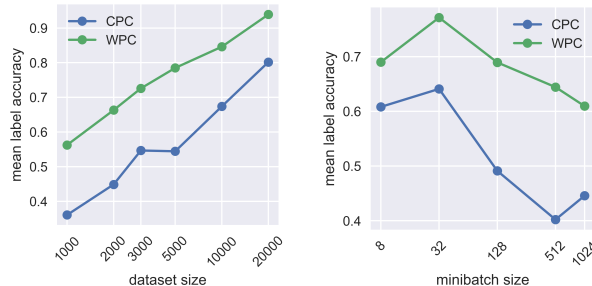


Figure 8. Performance of CPC and WPC on MultiviewShapes3D using convolutional neural networks. WPC performs consistently better than CPC over a range of dataset and minibatch sizes.

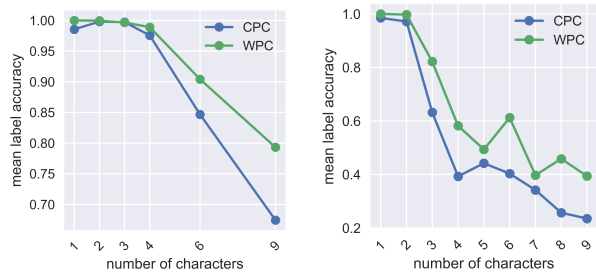


Figure 9. Performance of CPC and WPC on (a) SpatialMultiOmniglot and (b) StackedMultiOmniglot using convolutional neural networks. Even when using CNNs, large mutual information results in reduced performance for both CPC and WPC. WPC performs consistently better.

since they bring in their inductive biases such as translation invariance or invertibility via residual connections. Convnets also perform worse on StackedMultiOmniglot than SpatialMultiOmniglot, which is expected since SpatialMultiOmniglot arranges the Omniglot characters spatially which works well with convnet’s translation invariance. However, when the data does not match convnet’s inductive bias such as in StackedOmniglot, convnet performance suffers even more than fully connected networks. In this setting, WPC provides a larger improvement over CPC.

7. Conclusion

We proposed a new representation learning objective as an alternative to mutual information. This objective which we refer to as the Wasserstein dependency measure, uses the Wasserstein distance in place of KL divergence in mutual information. A practical implementations of this approach, Wasserstein predictive coding, is obtained by regularizing existing mutual information estimators to enforce Lipschitz continuity. We explore the fundamental limitations of prior mutual information-based estimators, present several problem settings where these limitations manifest themselves, resulting in poor representation learning performance, and show that WPC mitigates these issues to a large extent.

However, optimization of Lipschitz-continuous neural networks is still a challenging problem. Our results indicate that Lipschitz continuity is highly beneficial for representation learning, and an exciting direction for future work is to develop better techniques for enforcing Lipschitz continuity. As better regularization methods are developed, we expect the quality of representations learned via Wasserstein dependency measure to also improve.

Acknowledgement

The authors would like to thank Ben Poole, George Tucker, Alex Alemi, Alex Lamb, Aravind Srinivas, and Luke Metz for useful discussions and feedback on our research. SO is thankful to the Google Brain team for providing a productive and empowering research environment.

References

- Alain, G. and Bengio, Y. Understanding intermediate layers using linear classifier probes. *arXiv preprint arXiv:1610.01644*, 2016.
- Anil, C., Lucas, J., and Grosse, R. Sorting out lipschitz function approximation. *arXiv preprint arXiv:1811.05381*, 2018.
- Arjovsky, M., Chintala, S., and Bottou, L. Wasserstein gan. *arXiv preprint arXiv:1701.07875*, 2017.
- Atal, B. S. and Schroeder, M. R. Adaptive predictive coding of speech signals. *Bell System Technical Journal*, 49(8): 1973–1986, 1970.
- Aytar, Y., Pfaff, T., Budden, D., Paine, T. L., Wang, Z., and de Freitas, N. Playing hard exploration games by watching youtube. *arXiv preprint arXiv:1805.11592*, 2018.
- Becker, S. and Hinton, G. E. Self-organizing neural network that discovers surfaces in random-dot stereograms. *Nature*, 355(6356):161, 1992.
- Belghazi, M. I., Baratin, A., Rajeshwar, S., Ozair, S., Bengio, Y., Courville, A., and Hjelm, D. Mutual information neural estimation. In Dy, J. and Krause, A. (eds.), *Proceedings of the 35th International Conference on Machine Learning*, volume 80 of *Proceedings of Machine Learning Research*, pp. 531–540, Stockholmsmssan, Stockholm Sweden, 10–15 Jul 2018. PMLR. URL <http://proceedings.mlr.press/v80/belghazi18a.html>.
- Bell, A. J. and Sejnowski, T. J. An information-maximization approach to blind separation and blind deconvolution. *Neural computation*, 7(6):1129–1159, 1995.
- Brock, A., Donahue, J., and Simonyan, K. Large scale gan training for high fidelity natural image synthesis. *arXiv preprint arXiv:1809.11096*, 2018.
- Clark, A. Whatever next? predictive brains, situated agents, and the future of cognitive science. *Behavioral and brain sciences*, 36(3):181–204, 2013.
- Crooks, G. E. On measures of entropy and information. 2017.
- Devlin, J., Chang, M.-W., Lee, K., and Toutanova, K. Bert: Pre-training of deep bidirectional transformers for language understanding. *arXiv preprint arXiv:1810.04805*, 2018.
- Dinh, L., Sohl-Dickstein, J., and Bengio, S. Density estimation using real nvp. *arXiv preprint arXiv:1605.08803*, 2016.
- Doersch, C. and Zisserman, A. Multi-task self-supervised visual learning.
- Doersch, C., Gupta, A., and Efros, A. A. Unsupervised visual representation learning by context prediction. In *Proceedings of the IEEE International Conference on Computer Vision*, pp. 1422–1430, 2015.
- Donahue, J., Krähenbühl, P., and Darrell, T. Adversarial feature learning. *arXiv preprint arXiv:1605.09782*, 2016.
- Dumoulin, V., Belghazi, I., Poole, B., Mastropietro, O., Lamb, A., Arjovsky, M., and Courville, A. Adversarially learned inference. *arXiv preprint arXiv:1606.00704*, 2016.
- Dwibedi, D., Tompson, J., Lynch, C., and Sermanet, P. Learning actionable representations from visual observations. In *2018 IEEE/RSJ International Conference on Intelligent Robots and Systems (IROS)*, pp. 1577–1584. IEEE, 2018.
- Elias, P. Predictive coding–i. *IRE Transactions on Information Theory*, 1(1):16–24, 1955.
- Friston, K. and Kiebel, S. Predictive coding under the free-energy principle. *Philosophical Transactions of the Royal Society of London B: Biological Sciences*, 364(1521): 1211–1221, 2009.
- Gidaris, S., Singh, P., and Komodakis, N. Unsupervised representation learning by predicting image rotations. *arXiv preprint arXiv:1803.07728*, 2018.
- Goodfellow, I., Pouget-Abadie, J., Mirza, M., Xu, B., Warde-Farley, D., Ozair, S., Courville, A., and Bengio, Y. Generative adversarial nets. In *Advances in neural information processing systems*, pp. 2672–2680, 2014.
- Gulrajani, I., Ahmed, F., Arjovsky, M., Dumoulin, V., and Courville, A. C. Improved training of wasserstein gans. In *Advances in Neural Information Processing Systems*, pp. 5767–5777, 2017.
- Hjelm, R. D., Fedorov, A., Lavoie-Marchildon, S., Grewal, K., Trischler, A., and Bengio, Y. Learning deep representations by mutual information estimation and maximization. *arXiv preprint arXiv:1808.06670*, 2018.

- Jaderberg, M., Mnih, V., Czarnecki, W. M., Schaul, T., Leibo, J. Z., Silver, D., and Kavukcuoglu, K. Reinforcement learning with unsupervised auxiliary tasks. *arXiv preprint arXiv:1611.05397*, 2016.
- Kim, H. and Mnih, A. Disentangling by factorising. In Dy, J. and Krause, A. (eds.), *Proceedings of the 35th International Conference on Machine Learning*, volume 80 of *Proceedings of Machine Learning Research*, pp. 2649–2658, Stockholm, Sweden, 10–15 Jul 2018. PMLR. URL <http://proceedings.mlr.press/v80/kim18b.html>.
- Kim, H., Kim, J., Jeong, Y., Levine, S., and Song, H. O. Emi: Exploration with mutual information maximizing state and action embeddings. *arXiv preprint arXiv:1810.01176*, 2018.
- Kingma, D. P. and Welling, M. Auto-encoding variational bayes. *arXiv preprint arXiv:1312.6114*, 2013.
- Kingma, D. P., Salimans, T., Jozefowicz, R., Chen, X., Sutskever, I., and Welling, M. Improved variational inference with inverse autoregressive flow. In *Advances in neural information processing systems*, pp. 4743–4751, 2016.
- Kraskov, A., Stögbauer, H., and Grassberger, P. Estimating mutual information. *Physical review E*, 69(6):066138, 2004.
- Lake, B. M., Salakhutdinov, R., and Tenenbaum, J. B. Human-level concept learning through probabilistic program induction. *Science*, 350(6266):1332–1338, 2015.
- LeCun, Y., Bengio, Y., and Hinton, G. Deep learning. *nature*, 521(7553):436, 2015.
- Linsker, R. Self-organization in a perceptual network. *Computer*, 21(3):105–117, 1988.
- Liu, Z., Luo, P., Wang, X., and Tang, X. Deep learning face attributes in the wild. In *Proceedings of International Conference on Computer Vision (ICCV)*, 2015.
- McAllester, D. and Statos, K. Formal limitations on the measurement of mutual information. *arXiv preprint arXiv:1811.04251*, 2018.
- Miyato, T., Kataoka, T., Koyama, M., and Yoshida, Y. Spectral normalization for generative adversarial networks. *arXiv preprint arXiv:1802.05957*, 2018.
- Nemenman, I., Bialek, W., and van Steveninck, R. d. R. Entropy and information in neural spike trains: Progress on the sampling problem. *Physical Review E*, 69(5):056111, 2004.
- Neysshabur, B., Bhojanapalli, S., McAllester, D., and Srebro, N. A pac-bayesian approach to spectrally-normalized margin bounds for neural networks. *arXiv preprint arXiv:1707.09564*, 2017.
- Nguyen, X., Wainwright, M. J., and Jordan, M. I. Estimating divergence functionals and the likelihood ratio by convex risk minimization. *IEEE Transactions on Information Theory*, 56(11):5847–5861, 2010.
- Odena, A., Olah, C., and Shlens, J. Conditional image synthesis with auxiliary classifier gans. In *Proceedings of the 34th International Conference on Machine Learning - Volume 70, ICML’17*, pp. 2642–2651. JMLR.org, 2017. URL <http://dl.acm.org/citation.cfm?id=3305890.3305954>.
- Palmer, S. E., Marre, O., Berry, M. J., and Bialek, W. Predictive information in a sensory population. *Proceedings of the National Academy of Sciences*, 112(22):6908–6913, 2015.
- Peyré, G., Cuturi, M., et al. Computational optimal transport. Technical report, 2017.
- Poole, B., Ozair, S., Oord, A. v. d., Alemi, A., and Tucker, G. On variational lower bounds of mutual information. 2018.
- Radford, A., Narasimhan, K., Salimans, T., and Sutskever, I. Improving language understanding by generative pre-training. 2017.
- Rezende, D. J. and Mohamed, S. Variational inference with normalizing flows. *arXiv preprint arXiv:1505.05770*, 2015.
- Sermanet, P., Lynch, C., Chebotar, Y., Hsu, J., Jang, E., Schaal, S., and Levine, S. Time-contrastive networks: Self-supervised learning from video. *arXiv preprint arXiv:1704.06888*, 2017.
- Tkačik, G. and Bialek, W. Information processing in living systems. *Annual Review of Condensed Matter Physics*, 7: 89–117, 2016.
- van den Oord, A., Li, Y., and Vinyals, O. Representation learning with contrastive predictive coding. *arXiv preprint arXiv:1807.03748*, 2018.
- Villani, C. *Optimal transport: old and new*, volume 338. Springer Science & Business Media, 2008.
- Wei, D., Lim, J. J., Zisserman, A., and Freeman, W. T. Learning and using the arrow of time. In *The IEEE Conference on Computer Vision and Pattern Recognition (CVPR)*, June 2018.
- Zhang, R., Isola, P., and Efros, A. A. Colorful image colorization. In *ECCV*, 2016.